

A Broadband and Viales Vertical Microstrip-to-Microstrip Transition

Xiaobo Huang and Ke-Li Wu, *Fellow, IEEE*

Abstract—A novel, broadband, viales, and vertical microstrip-to-microstrip transition is proposed in this paper. The transition consists of two open-circuited microstrip resonators and a U-shaped resonant-slot on the common ground plane. A physics-based equivalent-circuit model is developed for interpreting its working mechanism and facilitating the design process. The transition is analogous to a three-pole resonator filter. Based on the equivalent-circuit model, the coupling coefficients of the physical circuit can be calculated from the group delay information of two segregated electromagnetic models. To effectively control the couplings, a modified configuration is also proposed. A prototype transition is designed using the proposed design formulas. The fabricated circuit is measured to validate the proposed transition and the equivalent-circuit model. Good agreement is obtained between not only the measured and the simulated performance, but also the designed and the extracted-circuit model. In addition to the wide bandwidth, the features of viales and easy fabrication make the novel transition very attractive for system-on-package applications.

Index Terms—Broadband, equivalent circuit, microstrip transitions, multilayer circuits.

I. INTRODUCTION

WIRELESS communication systems operating at microwave and millimeter-wave frequencies have been widely used for gigabit/second-rate data transmission of a point-to-point or a point-to-multipoint last-mile solution of wireless local area networks. The fast growing market for such a system drives the increasing demands of highly integrated subsystems and modules for the high-frequency bands. Similar to the integration technologies for RF frequency bands, due to the design flexibility, low manufacturing cost, and suitability for high-volume production 3-D multilayer integration technologies, such as wafer-level silicon-based heterogeneous chip technologies, silicon through-vias (TSVs), and vertical interconnection using low-temperature co-fired ceramic (LTCC), have drawn a great deal of attention from the industry for millimeter-wave and terahertz applications [1], [2].

Manuscript received July 19, 2011; revised January 10, 2012; accepted January 12, 2012. Date of publication February 24, 2012; date of current version April 04, 2012. This work was supported by the Research Grants Council of the Hong Kong Special Administrative Region, China under Grant 2150647.

X. Huang was with the Department of Electronic Engineering, The Chinese University of Hong Kong, Shatin, Hong Kong. He is now with the China Research and Development Center, Comba Telecommunication Systems, Guangzhou 510530, China (e-mail: xbhuang@ee.cuhk.edu.hk).

K.-L. Wu is with the Department of Electronic Engineering, The Chinese University of Hong Kong, Shatin, Hong Kong (e-mail: klwu@ee.cuhk.edu.hk).

Color versions of one or more of the figures in this paper are available online at <http://ieeexplore.ieee.org>.

Digital Object Identifier 10.1109/TMTT.2012.2185945

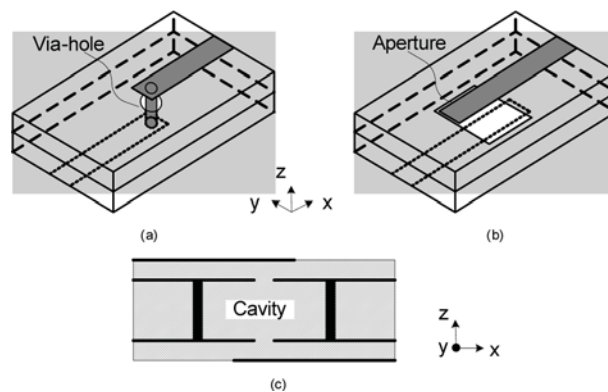


Fig. 1. Conventional configurations of microstrip-to-microstrip transitions. (a) Transition using a via-hole. (b) Aperture-coupled transition. (c) Cavity-coupled transition.

The large-scale integration of functional modules in a system-on-package (SOP) or a system-on-chip (SOC) module usually requires many vertical interconnections between multiple passive and active circuits and monolithic microwave integrated circuits (MMICs) built on different layers. In order to achieve a good electric performance, the interconnections should provide a very low insertion loss over a broad frequency bandwidth. Furthermore, the interconnection structures need to be easily fabricated. Traditionally, vertical via structures, shown in Fig. 1(a), are most commonly used in a 3-D integrated architecture [3]–[5]. However, a via-hole is a low-pass circuit and exhibits unwanted parasitic effects at high frequencies. Moreover, via-holes are not compatible with lithography-based etching processing for silicon-carrier-based millimeter-wave circuits. Enhanced bandwidth is obtained from the aperture-coupled transitions, as shown in Fig. 1(b), by changing the shape of the aperture or microstrip terminal [6]–[8]. These works are basically two-pole bandpass circuits. Moreover, no physically clear design guidelines are given for engineers to follow in these studies. Cavity-coupled transitions illustrated in Fig. 1(c) are proposed for transferring signals through several substrate layers [9]–[12]. As a matter of fact, the cavity can be regarded as an aperture in a thick common ground plane. Compared to the aperture-coupled transitions, the cavity-coupled type has a relatively narrower bandwidth due to only one cavity resonator between the two microstrip lines. On the other hand, the cavity has via-walls and the manufacturing difficulties are inevitable in via forming for high-frequency applications.

In this study, a novel viales configuration of a microstrip-to-microstrip transition for vertical interconnection is presented. The transition performs as a three-pole band-pass filter, which

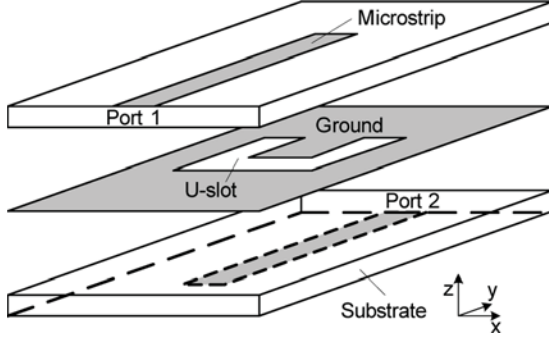


Fig. 2. Basic physical structure of the proposed transition.

creates three reflection zeros in the passband. An equivalent-circuit model is developed for interpreting the working mechanism of the proposed transition. The equivalent-circuit model reveals that the coupling coefficients of a physical transition circuit can be extracted by the group-delay information of two segregated sub-circuits. An optimal circuit model with realizable coupling coefficients can very well predict the electric performance and provide the design objectives for an accurate electromagnetic (EM) design. For further increasing the operating bandwidth, a modified structure of the transition is also presented and investigated to achieve the optimal bandwidth. For demonstrative purposes, a prototype of the proposed transition is designed at microwave band and fabricated to validate the equivalent-circuit model and the design formulas. Good agreement of the EM simulated and the measured results is obtained, which validates the proposed transition and illustrates the deterministic design procedure.

II. DESCRIPTION OF THE PROPOSED TRANSITION

Fig. 2 shows an exploded conceptual view of the basic structure of the proposed microstrip-to-microstrip transition. A more developed structure will be discussed in Section V for practical implementation. The transition consists of two open-circuited microstrip quarter-wavelength ($\lambda_g/4$) resonators, one of which is printed on the top of the upper substrate, the other, formed at the bottom of the lower substrate, and finally, a half wavelength U-shaped slotline resonator is etched on the common ground plane. The microstrip $\lambda_g/4$ resonators are placed perpendicularly to the middle section of the U-shaped slotline. The coupling between them can be controlled by the width of the slotline and an offset displacement from the center. The open ends are deliberately placed approximately $\lambda_g/4$ away from the middle section to create an open-circuited $\lambda_g/4$ resonator. In general, the couplings between the input/output microstrip lines and the $\lambda_g/4$ resonators are created by the discontinuity on the ground plane. In addition, the difference between the characteristic impedance of the input/output microstrip line and that of the open-circuited quarter-wavelength transmission line can also control the couplings. Therefore, based on the coupling arrangement, the operational principle of the transition can be well explained by the concept of a three-pole band-pass filter having

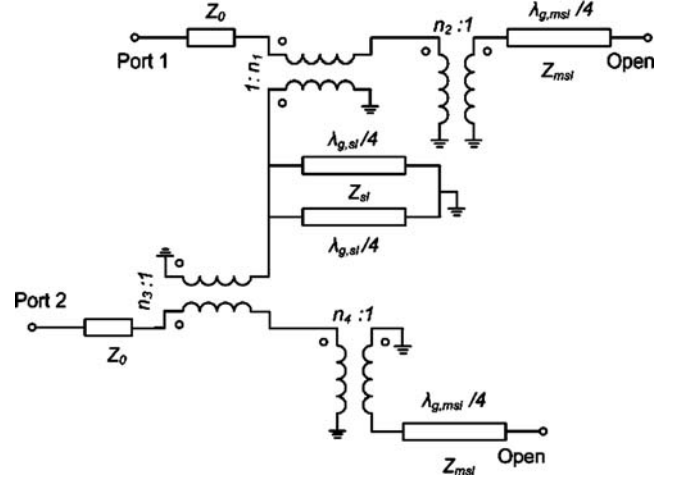


Fig. 3. Equivalent-circuit model of the proposed transition.

three reflection zeros in the passband. As compared to the published vialess microstrip-to-microstrip transitions of prior art, the proposed transition potentially provides a wider bandwidth.

III. WORKING PRINCIPLE AND EQUIVALENT-CIRCUIT MODEL

In order to illustrate the working mechanism of the transition, an equivalent-circuit model using transmission lines and ideal transformers is proposed in Fig. 3. The circuit model comprises four transformers, two open-circuited quarter-wavelength resonators and two shunt short-circuited quarter-wavelength resonators. The transformers in the circuit represent the EM couplings between the input/output transmission lines and the resonators. The U-shaped slot is represented by two parallel short-circuited quarter-wavelength slotline resonators. Specifically, transformers n_1 and n_3 represent the couplings between the U-shaped slotline resonator and the microstrip lines, while transformers n_2 and n_4 characterize the couplings between the open-circuited microstrip $\lambda_g/4$ resonators and the input and the output microstrip lines, respectively.

A. Coupling Coefficient for Open-Circuit Resonators

In the equivalent-circuit model shown in Fig. 3, there are four interlaced resonators: two open-circuited quarter-wavelength microstrip line resonators and a pair of shunt short-circuited slotline quarter-wavelength resonators. Having appropriately determined the dimensions of the four resonators for a given center frequency, designing the physical dimensions of a transition for realizing the four required coupling transformers, namely, n_1 , n_2 , n_3 , and n_4 will be critical.

It is known that an open-circuited quarter-wavelength microstrip line can be approximated by a series LC resonator circuit. Therefore, the coupling circuit of the input microstrip line and a $\lambda_g/4$ open-circuited resonator, as depicted in Fig. 4(a), can be represented by the lumped-element circuit of Fig. 4(b). Note that by definition of an ideal transformer with turns ratio n , there is $R' = R/n^2$, where R' is the resistance looking toward the transformer from the resonator and R is the source

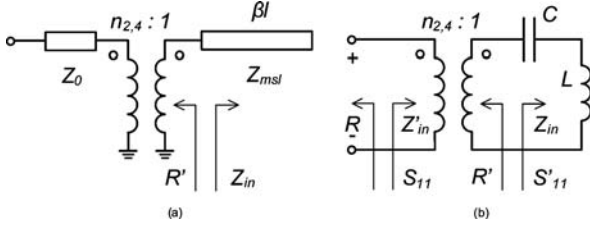


Fig. 4. (a) Coupling circuit between a transmission line and an open-circuited $\lambda/4$ resonator by an ideal transformer. (b) Corresponding lumped element circuit model of (a).

resistance, or the characteristic impedance Z_0 of the input microstrip line in the physical model. Therefore, the external Q of the LC series resonator circuit of Fig. 4(b) at the resonant frequency $\omega_0 = 1/\sqrt{LC}$ is

$$Q_e = \frac{\omega_0 L}{R'} = \sqrt{\frac{L}{C}} \cdot \frac{1}{R'} = n_{2,4}^2 \sqrt{\frac{L}{C}} \cdot \frac{1}{R} \quad (1)$$

where the notation $n_{2,4}$ refers to the coupling coefficient n_2 or n_4 .

For the quarter-wavelength open-circuited resonant circuit in Fig. 4(a), where $l = \lambda/4$, in the vicinity of resonant frequency $\omega = \omega_0 + \Delta\omega$ ($\Delta\omega \ll \omega_0$), the input impedance of the resonator

$$\begin{aligned} Z_{in} &= -jZ_{msl} \cot(\beta l) \\ &= -jZ_{msl} \cot\left(\frac{\pi}{2} + \frac{\pi\Delta\omega}{2\omega_0}\right) \\ &\approx jZ_{msl} \frac{\pi\Delta\omega}{2\omega_0} \end{aligned} \quad (2)$$

whereas its counterpart in the equivalent circuit of Fig. 4(b) looking into the LC series resonator can be expressed by

$$Z_{in} = j\omega_0 L \left(\frac{\omega_0 + \Delta\omega}{\omega_0} - \frac{\omega_0}{\omega_0 + \Delta\omega} \right) \approx j\omega_0 L \cdot \frac{2\Delta\omega}{\omega_0}. \quad (3)$$

Comparison of (2) to (3) leads to the inductance of the equivalent circuit

$$L = \frac{\pi Z_{msl}}{(4\omega_0)}. \quad (4)$$

Thus, (1) for the external Q reduces to

$$Q_e = n_{2,4}^2 \sqrt{\frac{L}{C}} \frac{1}{R} = \frac{n_{2,4}^2 \pi Z_{msl}}{4R}. \quad (5)$$

That is to say, if the external Q for the circuit in Fig. 4(a) can be measured from reflection coefficient S_{11} , for a set of predefined Z_{msl} and R , the coupling coefficient $n_{2,4}$ can then be extracted by (5).

By examining Fig. 4 and using the definition of an ideal transformer, the reflection coefficient looking at the input port of the microstrip line is given by

$$S_{11} = S'_{11} = \frac{Z_{in} - R'}{Z_{in} + R'} \text{ and } R' = \frac{R}{n_{2,4}^2}. \quad (6)$$

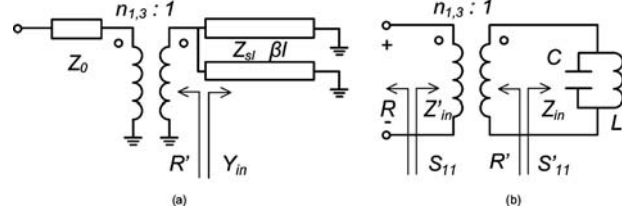


Fig. 5. (a) Coupling circuit between a transmission line and a pair of short-circuited shunt $\lambda/4$ resonators by an ideal transformer. (b) Corresponding lumped element circuit model of (a).

More specifically,

$$S_{11} = \frac{-jZ_{msl} \cot(\beta l) - \frac{\pi Z_{msl}}{4Q_e}}{-jZ_{msl} \cot(\beta l) + \frac{\pi Z_{msl}}{4Q_e}} = |S_{11}| e^{-2j\phi} \quad (7)$$

where $\phi = \tan^{-1}(\pi \tan(\beta l)/4Q_e)$.

It can be found that at resonance the group delay of the reflection coefficient is

$$\tau_{S_{11}}(\omega_0) = -\frac{\partial(-2\phi)}{\partial\omega} = \frac{4Q_e}{\omega_0}. \quad (8)$$

The above relation is not new and is valid for any single resonator circuit [13]. It is reexamined here for illustrative purposes. It can be seen that once Q_e is obtained from (8), the coupling coefficient $n_{2,4}$ can be determined by (5).

B. Coupling Coefficient for U-Shaped Slotline Resonator

At resonant frequency, the open-circuited quarter-wavelength resonators will short-circuit transformers 2 and 4 and the couplings $n_{1,3}$ and $n_{2,4}$ become isolated, where the notation $n_{1,3}$ refers to the coupling coefficient n_1 or n_3 . Thus, the coupling circuit between the microstrip line and the half-wavelength slotline resonator can be represented by an ideal transformer coupled to a pair of shunt short-circuited slotline resonators of length l , as shown in Fig. 5(a), whose input admittance is given by

$$Y_{in} = \frac{-j2 \cot(\beta l)}{Z_{sl}}. \quad (9)$$

Since a short-circuited quarter-wavelength transmission line can be approximated by a shunt LC circuit, the physical circuit of a transmission-line coupled half-wavelength U-shaped slotline resonator, which is abstracted by Fig. 5(a), can be represented by the lumped-element circuit of Fig. 5(b).

By a similar procedure as that for finding coupling coefficient $n_{2,4}$, it is straightforward to find that for the circuit of Fig. 5(b),

$$Q_e = \omega_0 C R' = \frac{\pi R'}{2Z_{sl}} = \frac{\pi R}{2n_{1,3}^2 Z_{sl}} \quad (10)$$

and that the group delay of the reflection coefficient is related to the external Q by (8).

From the above discussion, it can be seen that the U-shaped slot is an optimal geometry that is most pertinent to the circuit model, very convenient in controlling the couplings and small in footprint.

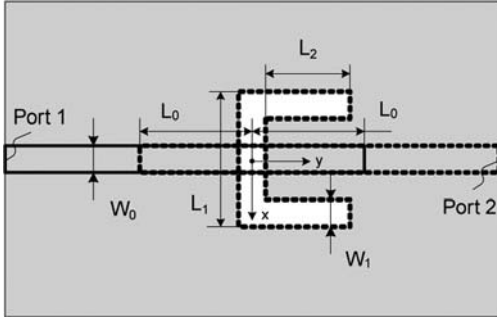


Fig. 6. Top view of the microstrip-to-microstrip transition.

IV. DESIGN GUIDELINES

Fig. 6 shows the top view of the proposed microstrip-to-microstrip transition, in which the related dimensional variables are also defined. The Zeland IE3D and Agilent ADS simulation software are used for EM simulation of the physical structure and circuit-model simulation of the proposed circuit model, respectively, in this study. The substrate used in this study is Rogers Duroid 5880 with dielectric constant of 2.22 and a thickness of 0.508 mm. The loss tangent of the material is 0.0009 and the thickness of the cladding copper is 0.017 mm. The design process starts with an optimal circuit model for the frequency band of interest, which can be obtained by a circuit-level simulator such as ADS with specified characteristic impedances and initial electrical lengths of the resonator stubs. Here, the characteristic impedances include those of I/O transmission lines and those of transmission line composing the resonators in the physical model; optimal electrical lengths determine the $\lambda_g/4$ resonators at appropriate resonance frequencies. Due to the simplicity of the equivalent-circuit model, it is a trivial task to optimize the circuit model that operates in the desired frequency bandwidth. The optimized circuit model should provide all the realizable coupling coefficients and serves as the coarse model in a space-mapping-like design process for the final physical model [14].

Usually a $50\text{-}\Omega$ microstrip line printed on the substrate is used for the I/O port and open-circuited quarter-wavelength resonators in the physical model. The total length of the U-shaped slotline resonator is designed to be a half guided wavelength. Changing the width of the slotline not only changes its characteristic impedance, but also affects its couplings to the I/O transmission lines. Fig. 7(a) and (b) shows the physical models for calculating coupling coefficients $n_{1,3}$ and $n_{2,4}$ in the equivalent circuit of Fig. 3, respectively.

Since at resonance the open-circuited quarter-wavelength resonator is nearly short circuited at the point extending to the U slotline resonator, in the model for calculating n_1 and n_3 , the microstrip line crossing-over the U slotline will be short-circuited to ground, as shown in Fig. 7(a). It can be seen from Fig. 7 that when calculating the coupling n_2 or n_4 , the U slotline resonator must be detuned so that no energy is divided. As the dominant factor for creating couplings n_2 and n_4 is the discontinuity of the slotline that divides the microstrip line and quarter-wavelength open-circuited resonator, one only needs to consider a short section of the slotline without taking the whole

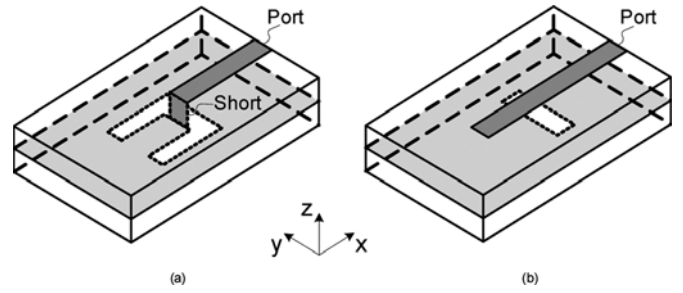


Fig. 7. Models for calculating the coupling coefficients. (a) For calculating n_1 or n_3 . (b) For calculating n_2 or n_4 .

U-shaped slotline resonator and the lower level microstrip line into consideration. In the proposed manner, all the coupling coefficients can be determined one by one independently by using the group-delay information of each corresponding EM model at the center frequency.

The initial dimensions of a transition can be obtained by the process given above. The final dimensions will be determined by a few steps of manual tuning using the concept of space-mapping optimization technique, which are: 1) EM simulation response of an unoptimized transition (fine model) is curve fitted by the response of corresponding circuit model described by Fig. 2 (coarse model); 2) the extracted-circuit model is compared to the optimized circuit model (golden template) for obtaining the error vector; and 3) a new EM simulation will be conducted using the updated fine model according to the error vector. The process will be repeated for a few numbers of iteration. Once the extracted-circuit model is close enough to the golden template, an optimized transition design is achieved.

V. BANDWIDTH ENHANCEMENT AND SIZE REDUCTION

In order to investigate the relationship between the couplings and the bandwidth, a parametric study based on the equivalent circuit shown in Fig. 3 is conducted. Fig. 8 shows the simulated return losses of the optimized circuit model with the variation of coupling coefficients n_1 and n_2 . For simplicity, the characteristic impedances at the two ports are $50\ \Omega$ and the electric length of each quarter-wavelength resonators is 90° at the center frequency of 7 GHz. Considering the symmetry of the circuit model, it is assumed that $n_1 = n_3$ and $n_2 = n_4$. It can be observed from Fig. 8 that as n_2 decreases while n_1 increases, the bandwidth will be enhanced greatly.

Although the proposed configuration provides three reflection zeros within the passband, the operating bandwidth of the physical model is limited by the U-shaped slot on the ground plane. As mentioned above, it is difficult for a single discontinuity to control all the required couplings. Therefore, a modified structure, as shown in Fig. 9, is proposed for a better control of couplings so that the bandwidth can be increased as broad as possible. It is noted that two stepped discontinuities are inserted between the I/O port and the open-circuited quarter-wavelength resonator. In principle, having the high- and low-impedance line section decreases the coupling n_2 that controls the power into the open-circuited quarter-wavelength resonators, while changing the width of slotline can increase the coupling coefficient n_1 that directs the signal to the U-shaped

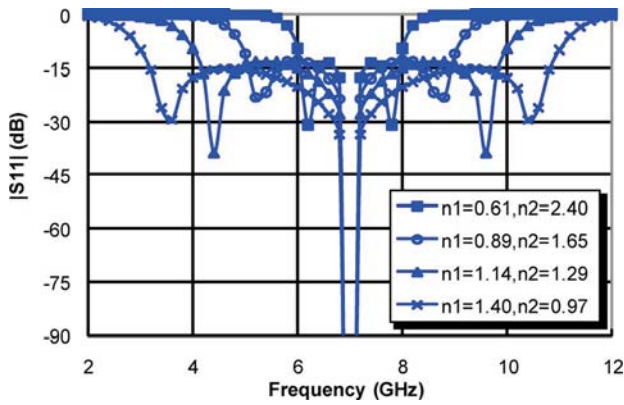


Fig. 8. Simulated responses of the circuit model with n_1 and n_2 as parameters.

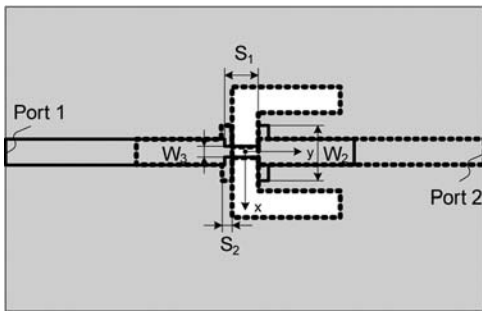


Fig. 9. Top view of the modified structure.

slotline resonator. Fig. 10 illustrates the relation between the coupling coefficient n_1 and the width of slotline. Fig. 11 shows the relation between the coupling n_2 and the width of the high-impedance line. It is observed that the coupling n_2 can be effectively reduced in this manner. On the other hand, the low-impedance discontinuity, as it provides a positive electrical length to the open-circuited quarter-wavelength resonator, makes the modified structure of the transition more compact, as compared to the original structure shown in Fig. 2. Fig. 12 shows the variation of resonance frequencies of the open-circuited quarter-wavelength resonator versus the width of the low-impedance line. It can be seen that using the modified structure can reduce the size of transition by about 18%. Thus, when determining the physical length of the resonator, this size reduction effect needs to be taken into consideration. By the way, during the determination of the coupling coefficients in the physical model, the corresponding stepped-impedance lines should be included in the EM model.

VI. EXPERIMENTAL VERIFICATION

By following the design procedure outlined in Section IV, one can easily design a circuit model of a transition provided that the characteristic impedances of each transmission-line resonator are given. As an example, the design procedure of a vertical microstrip-to-microstrip transition, as shown in Fig. 9, is employed here, where a 50-Ω microstrip line is used for both microstrip line and open-circuited quarter-wavelength resonator. The U-shaped slotline has a characteristic impedance of 127 Ω that is designed by the closed-form formulas given in [15].

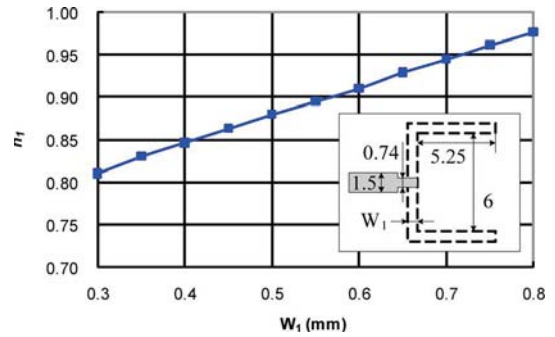


Fig. 10. Relation between the coupling coefficient n_1 and the width of slotline.

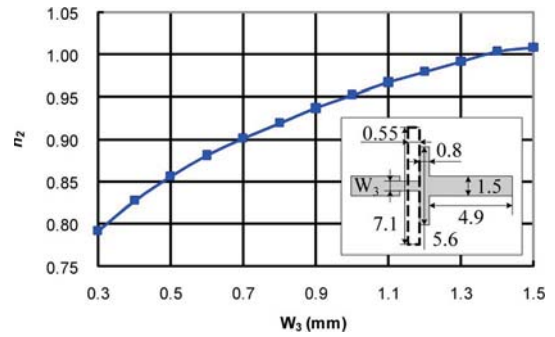


Fig. 11. Relation between the coupling coefficient n_2 and the width of inserted high-impedance line.

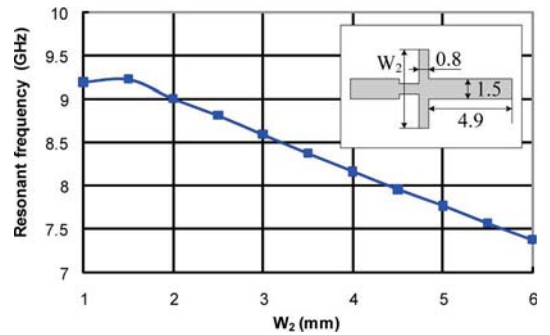


Fig. 12. Resonant frequency versus the width of the low-impedance line of the modified open-circuited quarter-wavelength resonator.

TABLE I
DIMENSIONS OF THE TRANSITION DESIGN EXAMPLE

Variables	Size (mm)	Variables	Size (mm)
W_0	1.50	L_0	5.96
W_1	0.55	L_1	7.10
W_2	5.60	L_2	5.25
W_3	0.74	S_1	1.00
		S_2	0.80

The final designed physical dimensions and the circuit model parameters of the transition are summarized in Tables I and II, respectively. Fig. 13 shows the simulated magnitudes of the S -parameters of the transition by the equivalent-circuit model and the EM designed model. The simulated results indicate that the transition has a more than 100% bandwidth for the

TABLE II
COMPARISON OF THE DESIGNED AND THE EXTRACTED-CIRCUIT MODEL PARAMETERS

Circuit Model Parameters	Optimal Designed	Extracted
n_1	0.896	0.868
n_2	0.909	0.884
f_0 of open-circuited $\lambda/4$ resonator	7.532 GHz	7.59 GHz
f_0 of parallel short-circuited $\lambda/4$ resonator	7.78 GHz	7.42 GHz

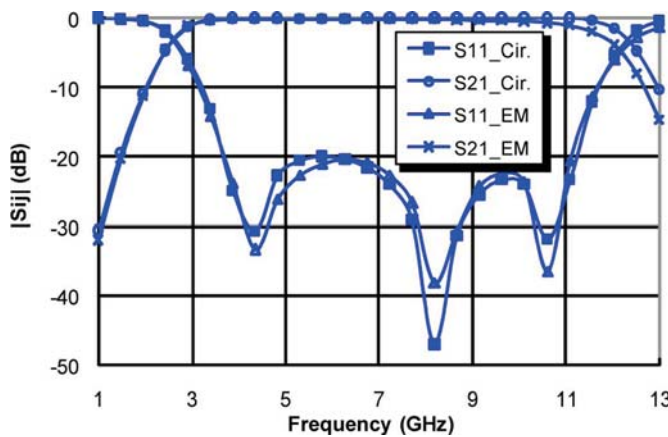


Fig. 13. Simulated results of the equivalent-circuit model and the EM model of a microstrip-to-microstrip transition.

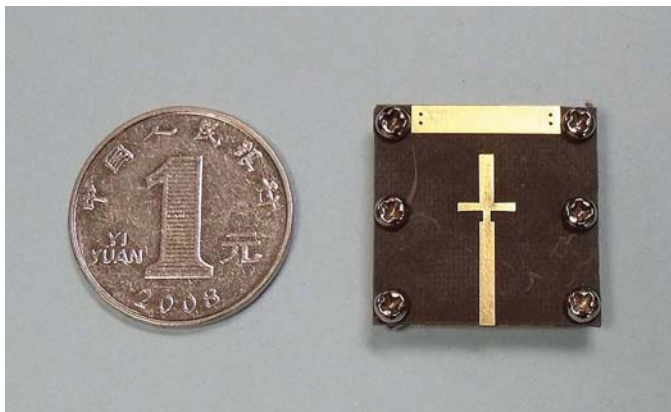


Fig. 14. Photograph of the prototype of a microstrip-to-microstrip transition.

return loss of better than 15 dB across the band with respect to the center frequency of 7.5 GHz. To verify the proposed circuit model and the design procedure, the final EM designed responses are curve fitted for extracting the corresponding circuit parameters according to the model proposed in Fig. 2. The extracted-circuit model parameters are also listed in Table II for comparative purpose. It is noted that agreement between the designed and the extracted coupling coefficients is excellent. The discrepancy in the resonance frequencies of the quarter-wavelength resonators is caused by the parasitic effects of the open end of the resonator and the parasitic effect of the bends of the U-shaped resonator. This verification demonstrates that proposed circuit model is fully competent for practical engineering designs.

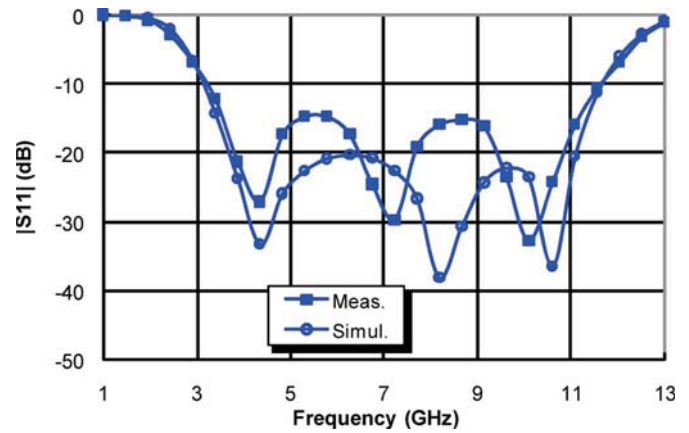


Fig. 15. Measured and simulated magnitudes of the reflection coefficients of the transition.

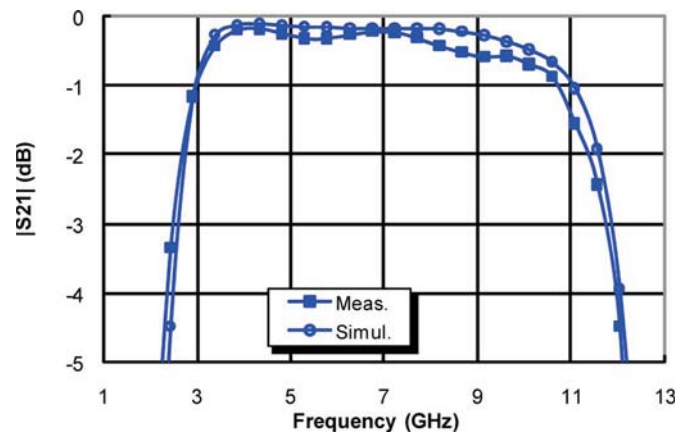


Fig. 16. Measured and simulated magnitudes of the transmission coefficients of the transition prototype.

TABLE III
DIMENSIONS OF THE TRANSITION DESIGN EXAMPLE

Reference	Return Loss	Bandwidth	Insertion Loss	Material
[7]	-8 dB	4 - 12 GHz	≤ 2.7 dB	N/A
[8]	-15 dB	4-10 GHz	≤ 0.9 dB	Rogers RO4003C
[12]	-15 dB	2.7 - 7.47 GHz	≤ 1 dB	Duroid 6010
This work	-15 dB	3.5 - 11.0 GHz	≤ 1.1 dB	Duroid 5880

In order to experimentally characterize the performance, a prototype of the designed transition is fabricated. The photograph of the prototype is shown in Fig. 14. The measurement is conducted by using an R&S ZVA67 vector network analyzer. Consequently, the measured and EM simulated magnitudes of the reflection and transmission coefficients are superimposed in Figs. 15 and 16, respectively. A very broad impedance-matching bandwidth of 3.1–11.56 GHz for a return loss less than 10 dB is achieved. The measured lowest insertion loss at the frequency of 7 GHz is about 0.25 dB. The measured results have demonstrated the excellent performance of the proposed transition.

To show the wide bandwidth feature of the proposed transition, as listed in Table III, its electric properties are compared

with those of some published representative microstrip-to-microstrip vertical vialess transitions in the similar frequency band. It should be noted that the bandwidth of a transition largely depends on the specified return-loss requirement and that the insertion loss strongly depends on the material used.

VII. CONCLUSION

A vialess, broadband, and vertical microstrip-to-microstrip transition using a U-shaped slot on their common ground plane has been presented in this paper. In contrast to conventional transition structures, the proposed transition provides three reflection zeros in the passband with low insertion loss over a very broad bandwidth. The working mechanism of the transition is interpreted by the concept of a three-pole resonator filter. An equivalent-circuit model of the transition is also developed as a coarse model for engineering design. Based on the equivalent circuit, design formula for the transition are also developed and demonstrated, with which the coupling coefficients can be determined by using group-delay information of two segregated simple EM models. In the end, a prototype transition is EM designed according to the proposed design equation and procedure and is fabricated to validate the proposed transition. It has been demonstrated that by following the design procedure, one can design a proposed broadband microstrip-to-microstrip transition in a deterministic way; and that the EM designed responses approach to the desired ones of the optimal circuit model very well. The EM simulated results indicate that a more than 100% bandwidth for the return loss of better than 15 dB across the band can be achieved. It can be foreseen that the proposed transition is particularly useful for broadband applications in the millimeter-wave frequency band and is highly suitable for multilayer wafer-level integration technologies, where making vias is difficult.

REFERENCES

- [1] S. M. Hu, L. Wang, Y.-Z. Xiong, T. G. Lim, B. Zhang, J. L. Shi, and X. J. Yuan, "TSV technology for millimeter-wave and terahertz design and applications," *IEEE Trans. Compon., Packag., Manuf. Technol.*, vol. 1, no. 2, pp. 12–21, Feb. 2011.
- [2] J.-H. Lee, G. Dejean, S. Sarkar, S. Pinel, K. Lim, J. Papapolymerou, J. Laskar, and M. M. Tentzeris, "Highly integrated millimeter-wave passive components using 3-D LTCC system-on-package (SOP) technology," *IEEE Trans. Microw. Theory Tech.*, vol. 53, no. 6, pp. 12–21, Jun. 2005.
- [3] M. Daneshmand, R. R. Mansour, P. Mousavi, S. Choi, B. Yassini, A. Zyburu, and M. Yu, "Integrated interconnect networks for RF switch matrix applications," *IEEE Trans. Microw. Theory Tech.*, vol. 53, no. 1, pp. 12–21, Jan. 2005.
- [4] R. Valois, D. Baillargeat, S. Verdyme, M. Lahti, and T. Jaakola, "High performances of shielded LTCC vertical transitions from DC up to 50 GHz," *IEEE Trans. Microw. Theory Tech.*, vol. 53, no. 6, pp. 2026–2032, Jun. 2005.
- [5] F. Casares-Miranda, C. Viereck, C. Camacho-Penñosa, and C. Caloz, "Vertical microstrip transition for multilayer microwave circuits with decoupled passive and active layers," *IEEE Microw. Wireless Compon. Lett.*, vol. 16, no. 7, pp. 401–403, Jul. 2006.
- [6] C. Chen, M. Tsai, and G. Alexopoulos, "Optimization of aperture transitions for multi-port microstrip circuits," *IEEE Trans. Microw. Theory Tech.*, vol. 44, no. 12, pp. 2457–2465, Dec. 1996.
- [7] L. Zhu and K. Wu, "Ultra broadband vertical transition for multilayer integrated circuits," *IEEE Microw. Guided Wave Lett.*, vol. 9, no. 11, pp. 453–455, Nov. 1999.
- [8] M. Abbosh, "Ultra wideband vertical microstrip-microstrip transition," *IET Microw. Antennas Propag.*, vol. 1, no. 5, pp. 968–972, Oct. 2007.
- [9] M. Tran and T. Itoh, "Analysis of microstrip lines coupled through an arbitrarily shaped aperture in a thick common ground plane," in *IEEE MTT-S Int. Microw. Symp. Dig.*, Atlanta, GA, 1993, vol. 3, pp. 819–822.
- [10] Lafond, M. Himdi, J. Daniel, and N. Haese-Rolland, "Microstrip/thick-slot/microstrip transitions in millimeter waves," *Microw. Opt. Technol. Lett.*, vol. 34, no. 2, pp. 100–103, Jul. 2002.
- [11] T. Swierczynski, D. McNamara, and M. Clenet, "Via-walled cavities as vertical transitions in multilayer millimeter-wave circuits," *Electron. Lett.*, vol. 39, no. 25, pp. 1829–1831, Dec. 2003.
- [12] Li, J. Cheng, and C. Lai, "Designs for broadband microstrip vertical transitions using cavity couplers," *IEEE Trans. Microw. Theory Tech.*, vol. 54, no. 1, pp. 464–472, Jan. 2006.
- [13] J. S. Hong and M. J. Lancaster, *Microstrip Filters for RF/Microwave Applications*. New York: Wiley, 2001, sec. 8.4.
- [14] J. W. Bandler, R. M. Biernacki, S. H. Chen, R. H. Hemmers, and K. Madsen, "Electromagnetic optimization exploiting aggressive space mapping," *IEEE Trans. Microw. Theory Tech.*, vol. 43, no. Dec., pp. 2874–2882, Dec. 1995.
- [15] R. Garg, P. Bhartia, I. Bahl, and A. Ittipaboon, *Microstrip Antenna Design Handbook*. Norwood, MA: Artech House, 2001, pp. 786–789.



Xiaobo Huang was born in Jiangsu, China, in 1983. He received the B.Eng. and M.Eng. degrees in electronic and optical engineering from the Nanjing University of Science and Technology, Nanjing, China, in 2005 and 2007, respectively, and the Ph.D. degree in electronic engineering from The Chinese University of Hong Kong, Shatin, Hong Kong, in 2011.

Since 2011, he has been a Research Engineer with the China Research and Development Center, Comba Telecommunication Systems, Guangzhou, China, where he is involved with LTE smart antennas. His current research interests include passive microwave and millimeter-wave circuits, antennas and filters for communication systems, and LTCC-based modules for wireless communications.



Ke-Li Wu (M'90–SM'96–F'11) received the B.S. and M.Eng. degrees from the Nanjing University of Science and Technology, Nanjing, China, in 1982 and 1985, respectively, and the Ph.D. degree from Laval University, Quebec, QC, Canada, in 1989.

From 1989 to 1993, he was with the Communications Research Laboratory, McMaster University, as a Research Engineer and a Group Manager. In March 1993, he joined the Corporate Research and Development Division, COM DEV International, where he was a Principal Member of Technical Staff. Since October 1999, he has been with The Chinese University of Hong Kong, Shatin, Hong Kong, where he is a Professor and the Director of the Radiofrequency Radiation Research Laboratory (R3L). He has authored or coauthored numerous publications in the areas of EM modeling and microwave and antenna engineering. His current research interests include partial element equivalent circuit (PEEC) and DPEC EM modeling of high-speed circuits, RF and microwave passive circuits and systems, synthesis theory and practices of microwave filters, antennas for wireless terminals, LTCC-based multichip modules (MCMs), and RF identification (RFID) technologies.

Dr. Wu is a member of IEEE MTT-8 Subcommittee (Filters and Passive Components) and is a Technical Program Committee (TPC) member for many international conferences including the IEEE Microwave Theory and Techniques Society (IEEE MTT-S) International Microwave Symposium (IMS). He was an associate editor for the IEEE TRANSACTIONS ON MICROWAVE THEORY AND TECHNIQUES (2006–2009). He was the recipient of the 1998 COM DEV Achievement Award for the development of exact EM design software of microwave filters and multiplexers and the 2008 Asia-Pacific Microwave Conference Prize.